The Effect of Loading Configuration and Footprint Geometry on Flexible Pavement Response Based on Linear Elastic Theory

Wael Alkasawneh* — Ernie Pan* — Roger Green**

** Dept. of Civil Engineering*
The University of Akron
Akron, OH 44325-3905, USA
Wael_alkasawneh@yahoo.com
pan2@uakron.edu

*** Ohio Department of Transportation*
1980 West Broad Street
Columbus, Ohio 43223, USA
Roger.Green@dot.state.oh.us

ABSTRACT. *The analysis of flexible pavements using circular footprint geometry with uniform contact pressure has been used for decades due to the lack of a powerful computational tool that is both reliable and simple to use by pavement engineers. In this paper, the effect of different footprint geometries with different loading configurations including nonuniform, uniform, and average pressures on the response of flexible pavement is investigated by varying the thickness of the AC layer. Our results indicate that the use of circular footprint areas with uniform contact pressure equal to the tire inflation pressure can produce erroneous results that tend to overestimate the predicted fatigue life and rutting life of flexible pavements. Therefore, the pavement response analysis should be carried out using the measured pressure and footprint area when possible. In addition, the results showed that elastic analysis of flexible pavement can be carried out reliably and accurately using advanced computational tools such as the multilayered elastic pavement program MultiSmart3D.*

KEYWORDS: *Multilayered Elastic Analysis, Flexible Pavement, Tire Contact Pressure, Tire Footprint.*

DOI:10.3166/RMPD.9.159-179

Road Materials and Pavement Design. Volume 9 – No. 2/2008, pages 159 to 179

1. Introduction

Pavement design requires good approximation of the anticipated stresses and strains within the pavement structure. The distribution of the tire contact pressure along the footprint area is very important since the distribution and the magnitude of the contact tire/pavement stresses influence the response of the pavement.

The contact pressures had been measured in the past using pressure transducers at different speeds to understand the factors that affect the tire/pavement contact pressure distribution (de Beer *et al.*, 1997). The results showed that the tire type, tire geometry, applied load, inflation pressure, and vehicle speed, affect the contact pressure distribution and the shape and size of the tire footprint area. For example, increasing the applied load on the tire can increase the pressure along the sides of the footprint area compared to the pressure within the footprint area. In addition, test results (de Beer et *al.*, 1997; Blab, 1999) indicated that, depending on the tire type and structure, reducing the inflation pressure by 50 percent can increase the footprint area by 42 percent, while increasing the inflation pressure in the tire by 50 percent can reduce the footprint area by 33 percent.

Tire footprint area has been modeled for years using a circular contact area and assuming that the tire/pavement contact stresses are equal to the inflation pressure of the tire. The footprint area is obtained normally by dividing the applied load on the tire by the tire inflation pressure as follows:

$$A_f = F/P \qquad [1]$$

where A_f is the footprint (contact) area, F is the applied load on tire, and P is the tire inflation pressure.

Equation [1] indicates that, when assuming a circular footprint area, reducing the inflation pressure by 50 percent can increase the footprint area by 100 percent while increasing the inflation pressure by 50 percent can reduce the footprint area by 33 percent. This example shows the strong effect of the inflation pressure on the footprint area as conventionally assumed. On the other hand, this example shows that the footprint area using this method can be different than the measured actual footprint area. In addition, test data from Luo and Prozzi (2005) indicated that the difference between the inflation pressure and the average contact stress over the footprint area was 18 percent, which contradicts the conventional assumption of equal pressures. This difference can be attributed to the distribution of the stresses within the tire itself and the tire carcass. Therefore, the assumption of having full pressure transfer of the tire pressure to the pavement should be further investigated for the benefit of pavement design.

Other typical tire footprint shapes that have been used to simulate the actual contact area are the rectangular and oval contact shapes. The circular shape has been

used for decades due to its simplicity when incorporated in any elastic analysis for layered flexible pavement system and the availability of closed form solutions. The rectangular and oval shapes are difficult to incorporate in elastic analysis due to the unmanageable complex expressions in the solution. Accurate selection of the tire contact area is always a challenge due to the difficulty of measuring the contact area for vehicles in motion and due to the wide range of tire types, inflation pressures, and tire boundary conditions such as the applied load, pavement surface roughness, and pavement temperature. In addition, simulation tools based on multilayered elastic theory that can be used in flexible pavement analysis are limited to the circular contact shape only while other advanced tools such as the finite element method are available for more complex contact geometries. However, Al-Qadi *et al.* (2004) showed that the size and thickness of the elements in the finite element model largely influence the analysis results and the associated computation time. No guidelines are available to choose the element size and thickness for pavement analysis and therefore several analysis trials should be carried out to achieve accurate and reasonable results, which can be both time consuming and error susceptible.

Finite element models have been developed using both finite and infinite elements to reduce the computation time of the flexible pavement analysis. Hjelmstad *et al.* (1997) showed that the location of the interface between the finite and the infinite elements should be determined based on trial and error and can affect both the computation time and accuracy. On the other hand, the contact pressure collection rate (the interval over which the contact pressure is measured) can increase the time needed to carry out the analysis using finite element models since finer mesh sizes at the surface of the pavement should be used to account for the irregular pressure distribution. Park *et al.* (2005) calibrated the size of the elements in the finite element model both vertically and horizontally using multilayered elastic analysis.

The effect of simplifying the tire contact area and pressure distribution within the contact area using either conventional geometrical shape or uniform pressure distribution should be investigated to provide guidelines for future analysis using the multilayer elastic theory.

2. Effect of tire contact area

It is known that pavement responses using numerical simulations are highly influenced by the tire-pavement interaction due to the simplification involved in simulating the tire pressure distribution on the pavement surface. Wang and Machemehl (2006) showed that using uniform tire-pavement pressure over an assumed circular tire footprint can overestimate the tensile strains at the bottom of the AC layer and underestimate the vertical compressive strains at the top of the subgrade. Yue and Svec (1995) showed that the distribution of the tire contact

pressure can mainly influence the stresses and deformations in the vicinity of the road surface while the responses of deeper layers depend mainly on the overall burden. Weissman (1999) showed that the assumption of a uniformly distributed pressure on a circular area can underestimate the stresses in the pavement. A three-dimensional finite element analysis was performed by Part *et al.* (2005) on nonuniform tire contact stresses and their results showed that the actual tire pressure distribution could significantly influence the pavement response.

In this paper, the effect of the tire contact area was studied by comparing the pavement response of several assumed contact areas with the response using the actually measured contact area and stresses. The flexible pavement response was calculated using the ***MultiSmart3D*** program. The MultiSmart3D program is a fast and accurate software tool developed by the Computer Modeling and Simulation Group at the University of Akron (Pan *et al.*, 2007), and it is based on the innovative computational and mathematical techniques for multilayered elastic systems (Pan, 1989a, 1989b, 1990, 1997). The MultiSmart3D program uses the propagator matrix method to solve only two systems of linear algebraic equations (4×4 and 2×2) no matter how many layers are in the pavement system. In addition, the adaptive Gauss quadrature is used along with an acceleration approach for fast and accurate calculation of integration. The program is capable of analyzing any pavement system regardless of the number of layers, the thickness of each layer, and the shape of the applied pressure at the surface of the pavement. Currently, the maximum number of layers that can be handled by existing layered programs is only 20, not to mention that these pavement programs cannot calculate the response of irregular loading shapes or configurations.

The typical flexible pavement section was summarized in Table 1 while a summary of the studied cases is shown in Table 2. The contact pressure at the surface of the pavement, as shown in Figure 1, was measured by Texas Department of Transportation (Luo and Prozzi, 2005). Pressure sensors were used to measure the tire-pavement contact stresses for different tire inflation pressures and loadings. The tire inflation pressure was 690 kPa acting on a circle with a diameter of 220.3 mm while the applied load was 26.3 kN (Luo and Prozzi, 2005). Pavement responses below the center of the contact pressure area were calculated using the MultiSmart3D program. The coordinate system is chosen such that the x- and y-axes are on the surface of the pavement ($z = 0$) whilst the z-axis is vertical to the x-y plane and extends along the depth direction.

In this study, the pavement response using the measured contact area within a rectangle with the measured contact pressure (Case 1) was compared to the response using several assumed regular contact areas including circular, rectangular, square, and oval contact areas (Cases 2 through 5). The pressure acting on the regular contact areas was assumed to equal the inflation pressure (uniform pressure) of the tire as typically used by engineers while the size of the contact area was controlled by Equation [1]. In addition, another case (Case 6) was analyzed using the measured

contact area (rectangle) but with a uniform pressure distribution equal to the average of the measured nonuniform pressure.

Table 1. *Parameters of a typical flexible pavement example*

Layer	Thickness (mm)	Resilient Modulus (MPa)	Poisson's Ratio
AC Layer	25.4,50.8,76.2,101.6, 127,152.4,177.8, 203.2,228.6,254,279.4, 304.8	3500	0.3
Base Layer	250	700	0.3
Subbase Layer	250	300	0.3
Subgrade Layer	Infinite Half-Space	100	0.3

Table 2. *Load configurations and footprint geometries*

Case No.	Load Configuration	Footprint Geometry
Case 1*	Nonuniform-Measured	Irregular
Case 2	Uniform-Tire Pressure	Rectangular
Case 3	Uniform-Tire Pressure	Square
Case 4	Uniform-Tire Pressure	Oval
Case 5	Uniform-Tire Pressure	Circular
Case 6	Uniform-Average Measured	Rectangular

* Case 1 is used as the reference case in this study.

Figure 2 shows the dimensions of the studied contact areas. The dimensions of the rectangle were assumed based on the approximation of the dimensions of the measured contact area. The square area was added as a special case of the rectangular contact area when the ratio between the length and width is equal to one. The oval contact area dimensions were suggested by Yoder and Witczak (1974).

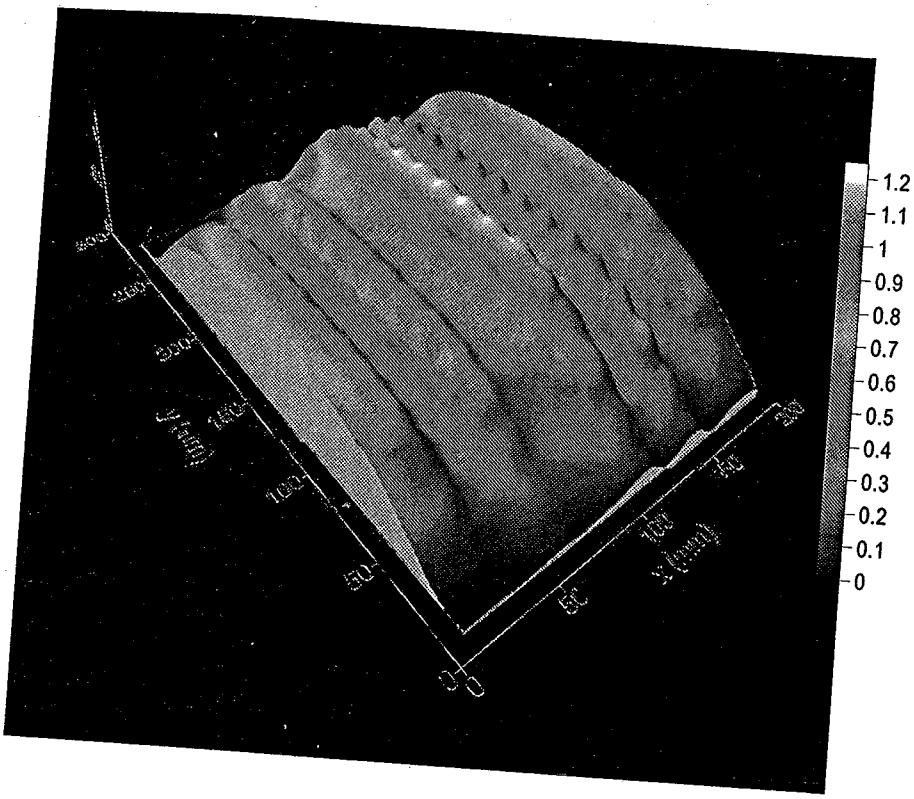

Figure 1. *Measured nonuniform tire pressure distribution (in MPa)*

The relation between the dimensions and the contact area for each of the studied shapes is given below:

Square $$L = \sqrt{A_f} \quad [2]$$

Rectangle $$L = \sqrt{1.4286 A_f} \quad [3]$$

Oval $$L = \sqrt{1.9131 A_f} \quad [4]$$

where A_f is the footprint (contact) area as calculated using Equation [1], and L is the dimension as shown in Figure 2.

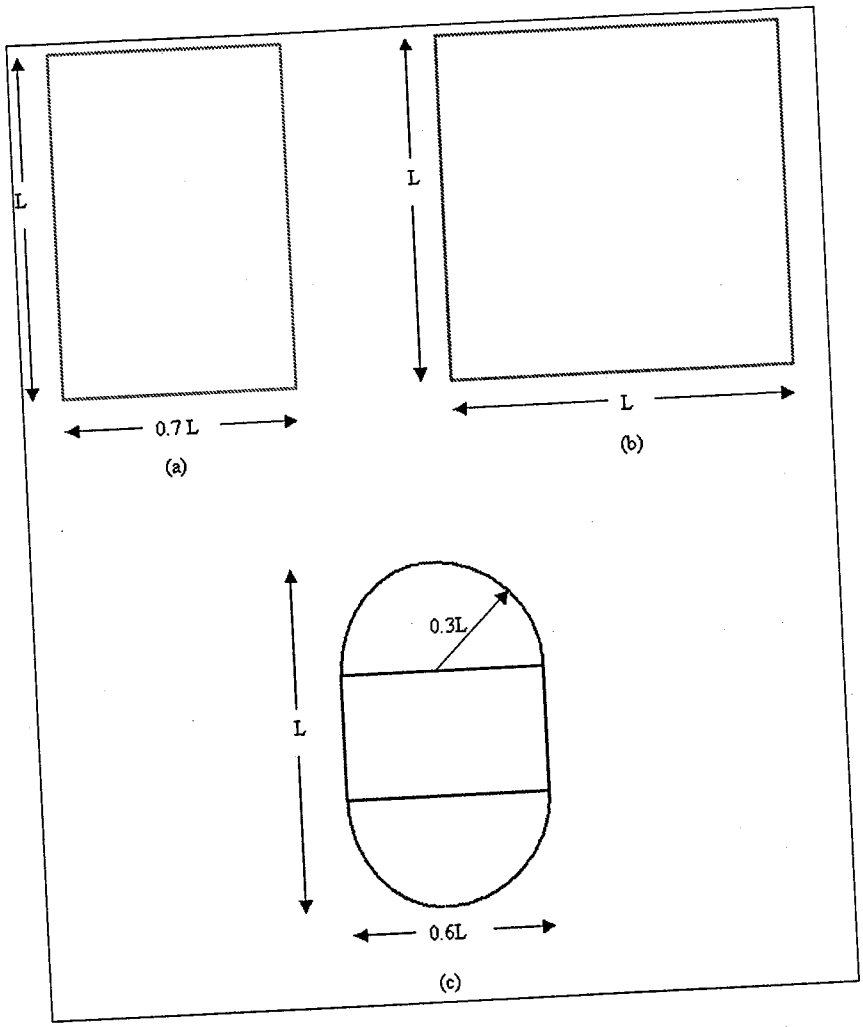

Figure 2. *Studied contact areas: (a) rectangular (Cases 2 and 6), (b) square (Case 3), and (c) oval (Case 4)*

In order to study the effect of the contact area shape and pressure distribution on the pavement response, the thickness of the asphalt concrete (AC) layer was varied between 25.4 mm (1 inch) and 304.8 mm (12 inches), as shown in Table 1. The studied AC thickness range includes both thin (less than 101.6 mm) and thick pavement layers.

2.1. *Pavement fatigue prediction*

The damage of flexible pavements can be assessed by predicting the number of loads needed to initiate cracks (fatigue cracking). The Shell Model (Bonnaure *et al.*,

1980) and the Asphalt Institute Model (Shook *et al.*, 1982) are frequently used for fatigue cracking in flexible pavements.

The Shell Model is based on two different loading modes, as given by Shell Constant Strain Model:

$$N_{\varepsilon} = 13909 A_f K \left(\frac{1}{\varepsilon_t}\right)^5 E_s^{-1.8} \quad [5]$$

and Shell Constant Stress Model:

$$N_{\sigma} = A_f K \left(\frac{1}{\varepsilon_t}\right)^5 E_s^{-1.4} \quad [6]$$

where N_{ε} and N_{σ} are the number of load repetitions to fatigue cracking using the constant strain and constant stress analysis, respectively, A_f and K are constants based on the material properties, ε_t is the tensile strain at the critical location and E_s is the stiffness of the material (*i.e.* resilient modulus). The constant strain model is applicable to thin asphalt pavement layers usually less than 51 mm, whilst the constant stress model is applicable to thick asphalt pavement layers usually more than 203 mm. The Shell Model was calibrated and generalized for any thickness as given below (MEPDG, 2004):

$$N_f = A_f K F'' \left(\frac{1}{\varepsilon_t}\right)^5 E_s^{-1.4} \quad [7]$$

where N_f is the number of load repetitions to fatigue cracking, F'' is a constant that depends on the layer thickness and the stiffness of the material.

The Asphalt Institute Model is given below:

$$N_f = 0.00432 C \left(\frac{1}{\varepsilon_t}\right)^{3.291} \left(\frac{1}{E_s}\right)^{0.854} \quad [8]$$

where, similarly, N_f is the number of load repetitions to fatigue cracking, C is a constant depending on the material properties, ε_t is the tensile strain at the critical location and again E_s is the stiffness of the material. The Asphalt Institute Model can be used for any thickness.

It can be seen from the above equations, that the critical tensile strain and the stiffness of the asphalt concrete layer are the main factors affecting the number of

load repetitions needed to initiate fatigue failure. The effect of the contact area and pressure distribution on the fatigue in flexible pavements can be studied by finding the ratio between the estimated number of repeated loads (N_f) from the calculated pavement response using the assumed contact area and pressure and that using the measured contact area and pressure. In other words, the ratio is equal to N_f (assumed area and pressure) over N_f (measured area and pressure).

2.2. *Rutting damage*

Rutting in flexible pavement is considered as a functional deterioration. Rutting is mainly predicted by calculating the vertical strains at the top of the subgrade and then estimating the allowable load repetitions until a certain rutting threshold is met. For example, Shook *et al.* (1982) assumed a rutting depth of 10 mm in their method, while Potter and Donald (1985) assumed a 20-30 mm rutting depth.

Recently, the results from the test sections at MnROAD were used to develop a method to predict the number of allowable load repetitions until rutting failure using a rutting depth of 13 mm as shown in the following relation (Skok *et al.*, 2003):

$$N_r = (5.5).10^{15}\left(\frac{1}{\varepsilon_v}\right)^{3.929} \quad [9]$$

where N_r is the number of allowable load repetitions until rutting failure, and ε_v is the maximum compressive strain at the top of the subgrade layer.

It can be seen, from the above equation, that the vertical strain at the top of the subgrade layer is very important to predict the lifetime of the pavement due to rutting. Similar to the fatigue case, the effect of the contact area and pressure distribution on the rutting can be studied by finding the ratio between the estimated number of repeated loads (N_r) from the calculated pavement response using the assumed contact area and pressure and that using the measured contact area and pressure. In other words, the ratio is equal to N_r (assumed area and pressure) over N_r (measured area and pressure).

3. Pavement response

The pavement response was studied for different cases as summarized in Table 1 using different loading and footprint configurations. In order to study the variation of the pavement response under different conditions the analysis results for the 50.8 mm AC layer (2 inches AC layer) and the 203.2 mm (8 inches AC layer) are shown in Figures 3 and 4.

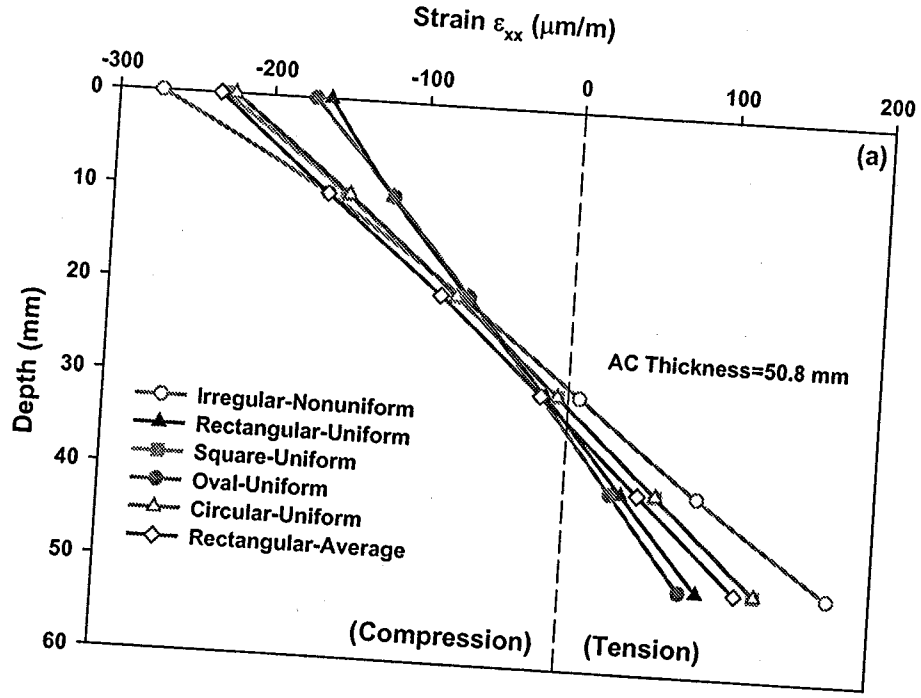
Strain ε_{xx} (μm/m)
-300
-200
-100
0
100
200
0
10
20
30
40
50
60
Depth (mm)
(a)
AC Thickness=50.8 mm
Irregular-Nonuniform
Rectangular-Uniform
Square-Uniform
Oval-Uniform
Circular-Uniform
Rectangular-Average
(Compression)
(Tension)

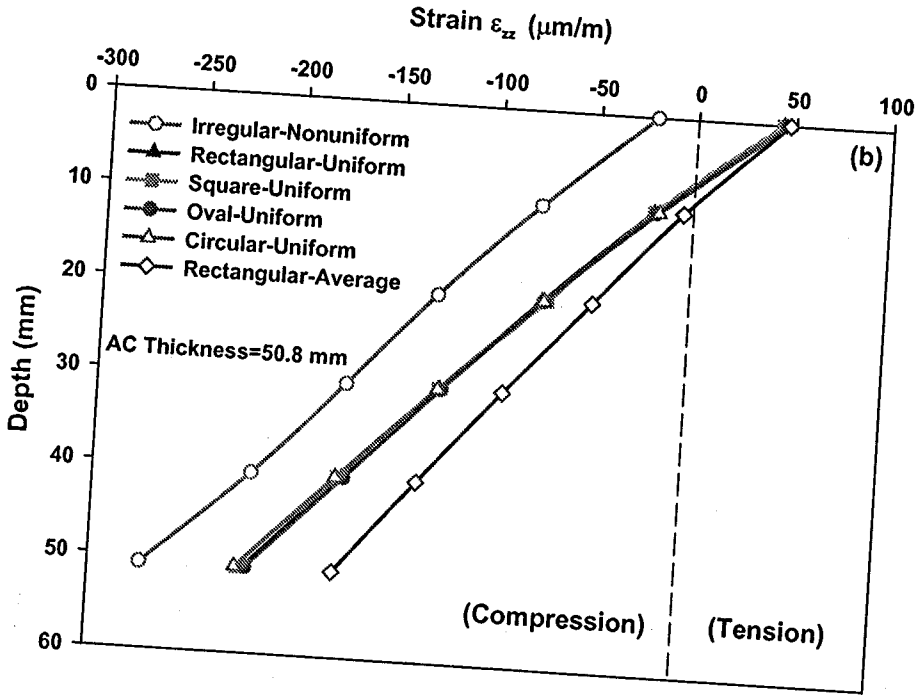
Strain ε_{zz} (μm/m)
-300
-250
-200
-150
-100
-50
0
50
100
0
10
20
30
40
50
60
Depth (mm)
(b)
Irregular-Nonuniform
Rectangular-Uniform
Square-Uniform
Oval-Uniform
Circular-Uniform
Rectangular-Average
AC Thickness=50.8 mm
(Compression)
(Tension)

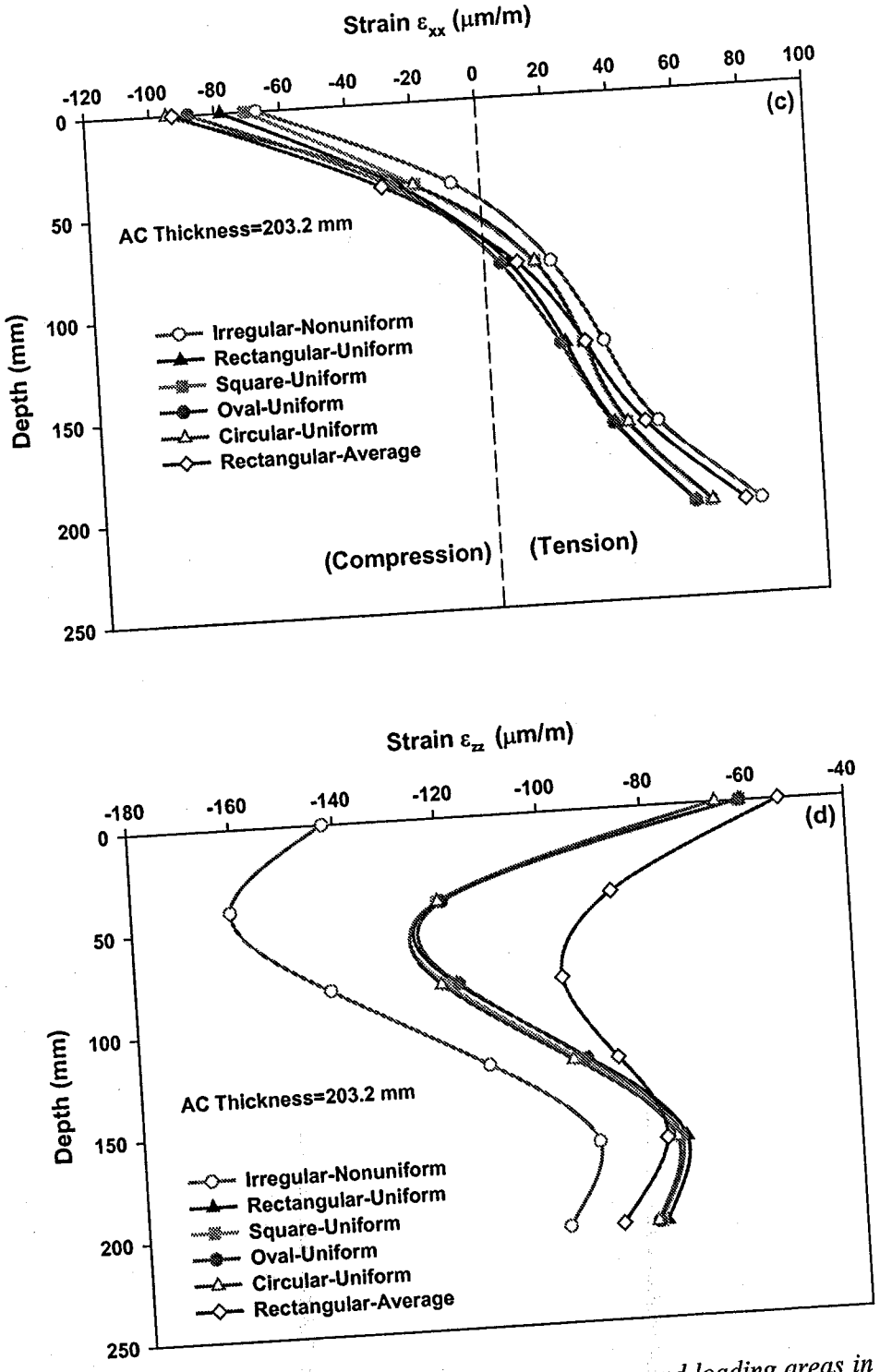

Figure 3. *Pavement response under different pressures and loading areas in a 50.8 mm AC layer: (a) horizontal strain ε_{xx}, (b) vertical strain ε_{zz}; and a 203.2 mm AC layer: (c) horizontal strain ε_{xx}, (d) vertical strain ε_{zz}*

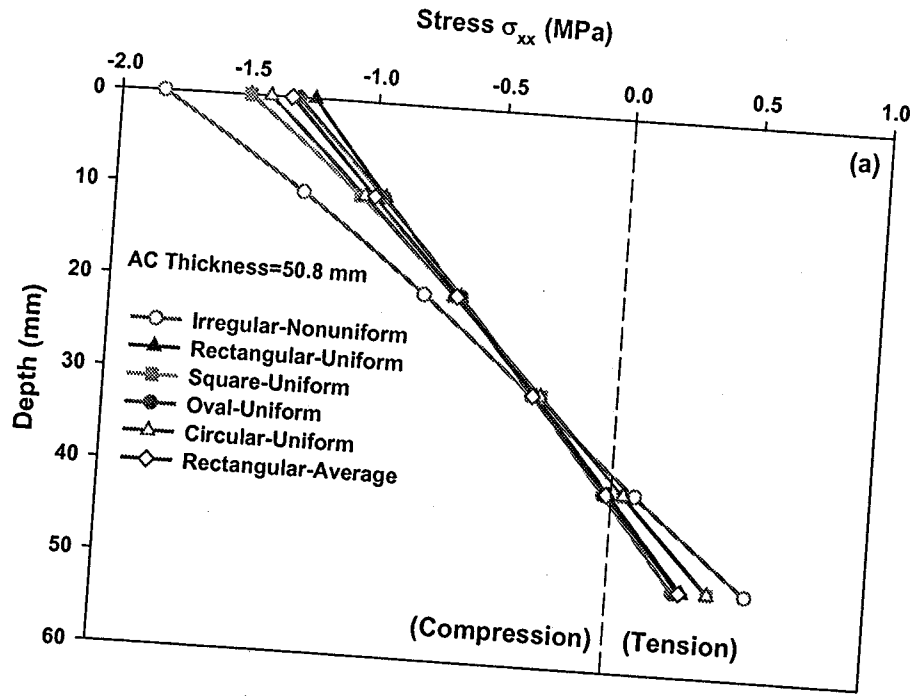
Stress σ_{xx} (MPa)
-2.0
-1.5
-1.0
-0.5
0.0
0.5
1.0
0
10
20
30
40
50
60
Depth (mm)
(a)
AC Thickness=50.8 mm
Irregular-Nonuniform
Rectangular-Uniform
Square-Uniform
Oval-Uniform
Circular-Uniform
Rectangular-Average
(Compression)
(Tension)

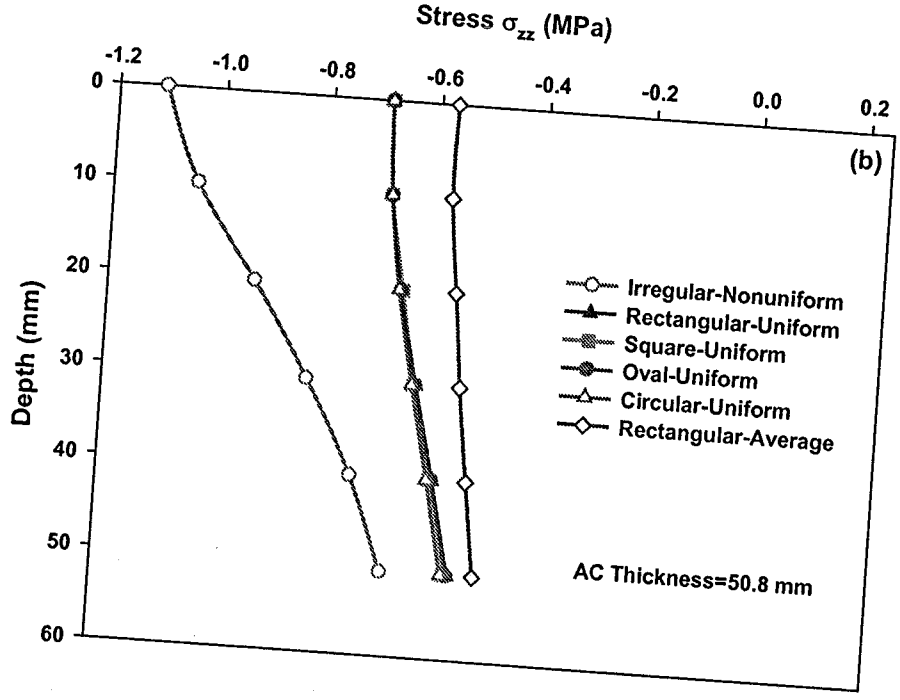
Stress σ_{zz} (MPa)
-1.2
-1.0
-0.8
-0.6
-0.4
-0.2
0.0
0.2
0
10
20
30
40
50
60
Depth (mm)
(b)
Irregular-Nonuniform
Rectangular-Uniform
Square-Uniform
Oval-Uniform
Circular-Uniform
Rectangular-Average
AC Thickness=50.8 mm

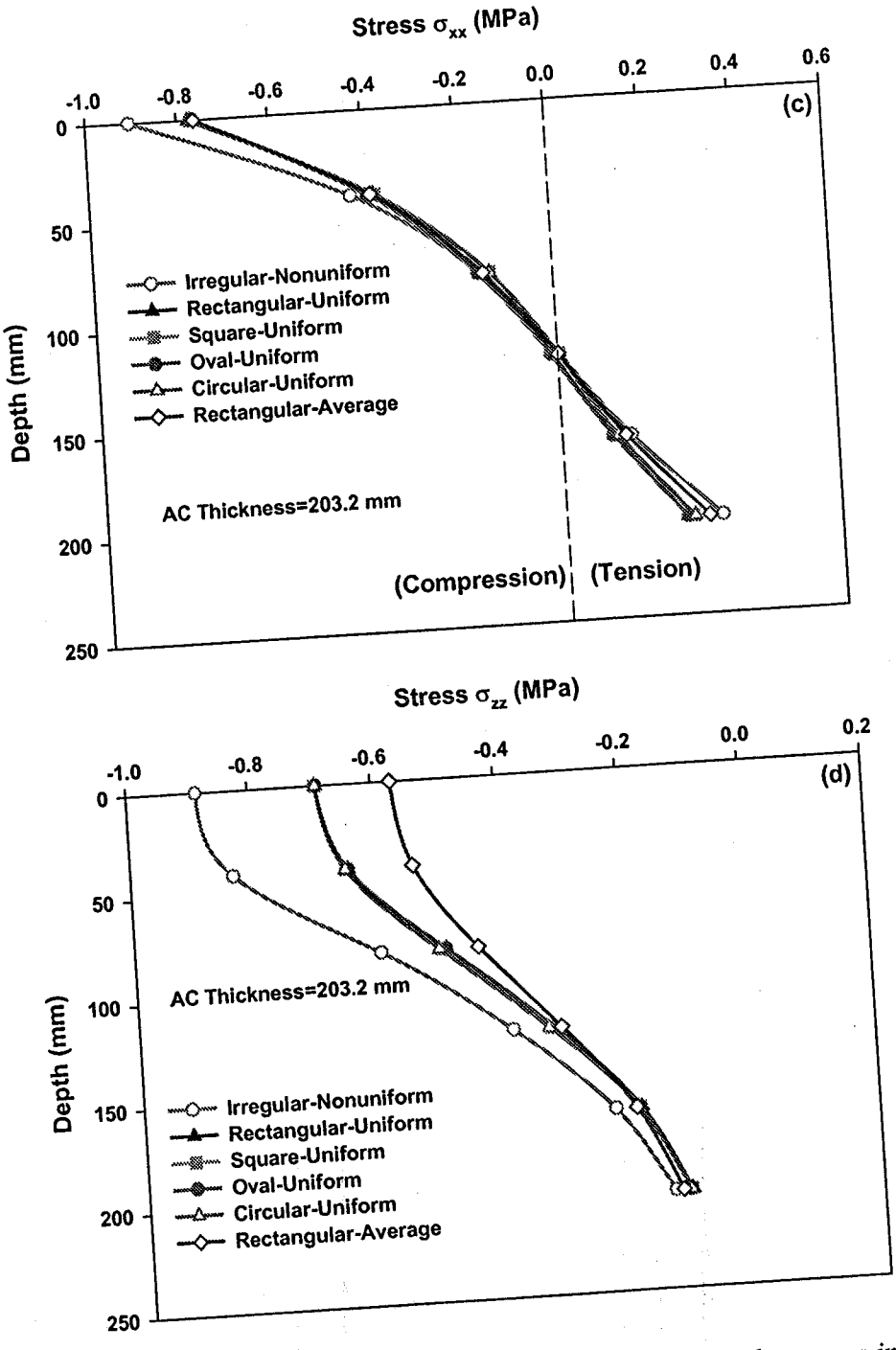

Figure 4. *Pavement response under different pressures and loading areas in a 50.8 mm AC layer: (a horizontal stress σ_{xx}, (b) vertical stress σ_{zz}; and a 203.2 mm AC layer: (c) horizontal stress σ_{xx}, (d) vertical stress σ_{zz}*

It can be seen from Figure 3 that the variation of the horizontal and vertical strains is nearly linear with depth in the thin AC layer (Figures 3a, 3b) while it is obviously nonlinear in the thick AC layer (Figures 3c, 3d) regardless of the loading configuration and footprint geometry. However, the selection of the loading configuration and footprint geometry tends to affect the calculated strains within the AC layer. The use of any footprint geometry or load configuration other than the measured ones underestimated the horizontal and vertical strains at the top and bottom of the thin AC layer (Figures 3a, 3b) while it overestimated the horizontal strain at the top of the thick AC layer and underestimated the horizontal strains at the bottom of the thick AC layer (Figure 3c). The vertical strains in the thick AC layer (Figure 3d) were always underestimated using the assumed geometries and loading configurations. In addition, increasing the AC layer thickness decreased the horizontal strains in the AC layer while it increased the vertical strains at the top of the AC layer and decreased the vertical strains at the bottom of the layer.

It is also interesting to observe that the measured load configuration and footprint area resulted in compressive vertical strains at the top and bottom of the thin AC layer while all other cases produced tensile vertical strains at the top of the thin AC layer and compressive vertical strains at the bottom of the thin AC layer (Figure 3b). On the other hand, only compressive vertical strains are predicted in the thick AC layer for all the six different cases (Figure 3d).

Figure 4 show the variation of the horizontal (Figures 4a, 4c) and vertical (Figures 4b, 4d) stresses for Cases 1 through 6 in thin and thick AC layers. The results indicate that Cases 2 through 5 produced relatively the same vertical stresses compared to each other while Case 6 produced different vertical stresses since the average measured contact pressure (569 kPa) in Case 6 was less than the tire pressure (690 kPa). However, the effect of the loading configuration and footprint area on the vertical stresses decreases as the depth in the thick AC layer increases (Figures 4c, 4d).

The effect of the loading configuration and footprint area showed negligible effect on the horizontal stresses in the thick AC layer (Figure 4c) while it showed relatively large variations at the top of the thin AC layer (Figure 4a). In all cases, the assumed load configuration and footprint area failed to produce reasonable results compared to those calculated using the measured loads and geometry.

The effect of the AC layer thickness on the response of the underlying layers was shown in Figures 5 and 6 for Case 1. These figures show, as anticipated, that more strains are transferred to the underlying layers through the AC layer as the thickness of the AC layer decreases. However, in thin AC layers the vertical strains increase with depth within the AC layer then decrease in the underlying layers (base, subbase, and subgrade layers) which can be attributed to the relatively low rigidity of the thin AC layer compared to the underlying layer. In general, the horizontal strains decreased with depth and with increasing thickness of the AC layer (Figure 5).

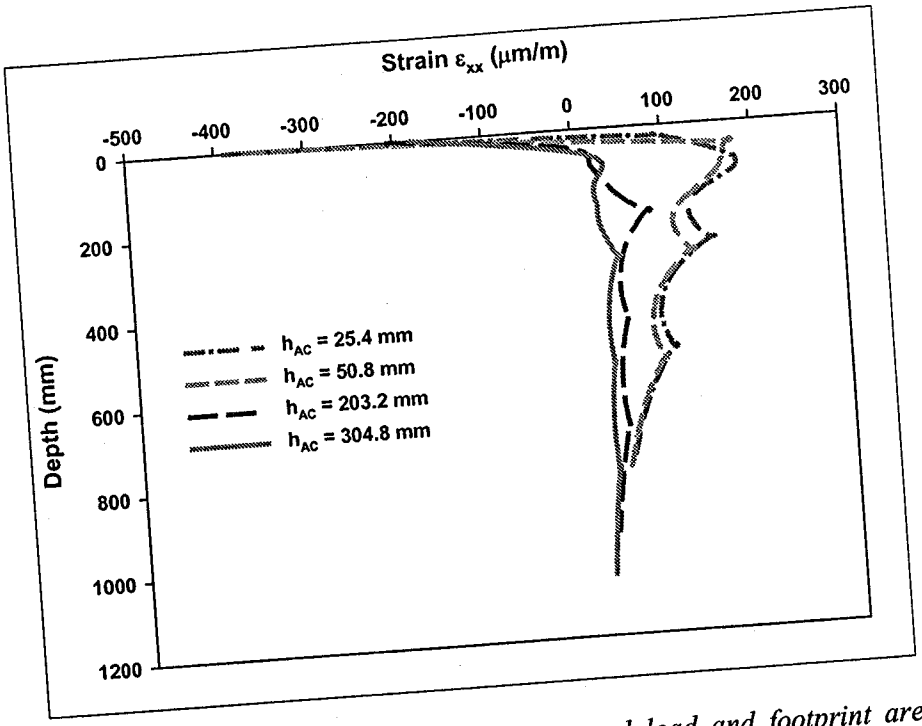

Figure 5. *Horizontal strain ε_{xx} under the measured load and footprint area for different AC layer thicknesses (Case 1)*

Understanding the variation of the horizontal strains at the bottom of the AC layer will help in understanding the effect of the calculated strains on the fatigue cracking prediction using Equations 7 and 8. As it can be seen in Figure 7, the horizontal strain at the bottom of the AC layer increases as the thickness of the AC layer increases to an optimal point. Then it decreases with increasing thickness for all the six different cases. However, the selection of the loading configuration and geometry influences the mechanical response along the bottom of the thin AC layers. Figure 7 shows that the horizontal strains at the bottom of the 25.4 mm AC layer are compressive for Cases 2, 4, and 6 while they are tensile for the other cases, indicating the invalidity of using Cases 2, 4, and 6 to study the pavement response in thin AC layers for fatigue cracking prediction. On the other hand, for AC layers with thickness larger than 152.4 mm (6 inches), Case 6 showed relatively close agreement (less than 9 percent difference) with Case 1 (measured case). For all cases, the horizontal strains at the bottom of the AC layer were underestimated compared to Case 1.

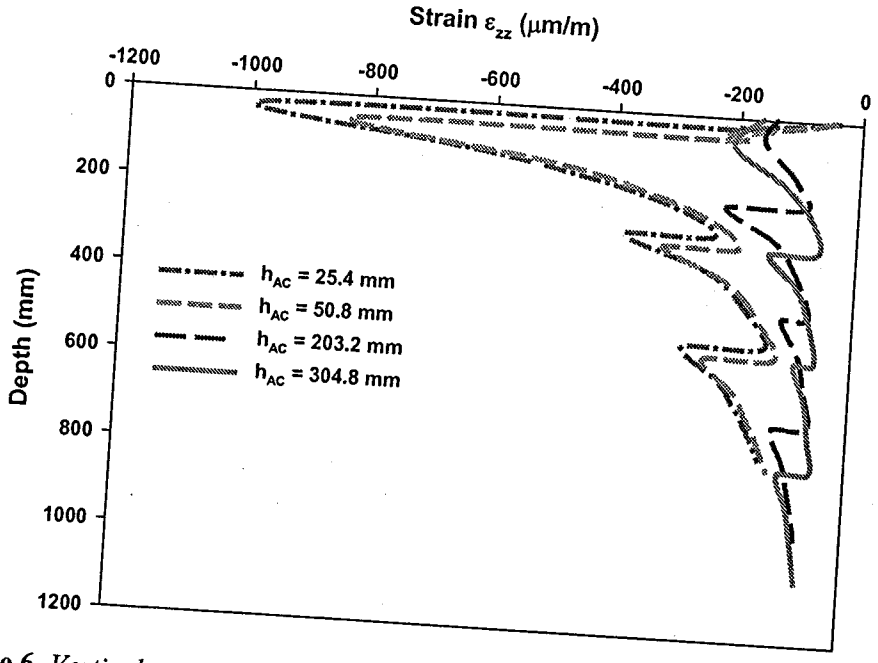

Figure 6. *Vertical strain ε_{zz} under the measured load and footprint area for different AC layer thicknesses (Case 1)*

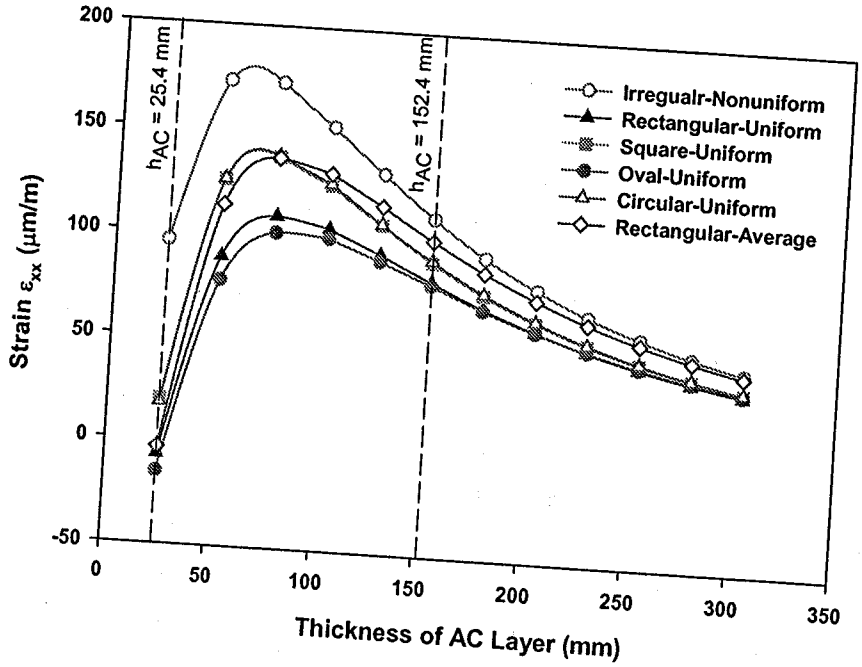

Figure 7. *Horizontal strain ε_{xx} at the bottom of the AC layer as a function of the AC layer thickness for different loading configurations and footprint areas*

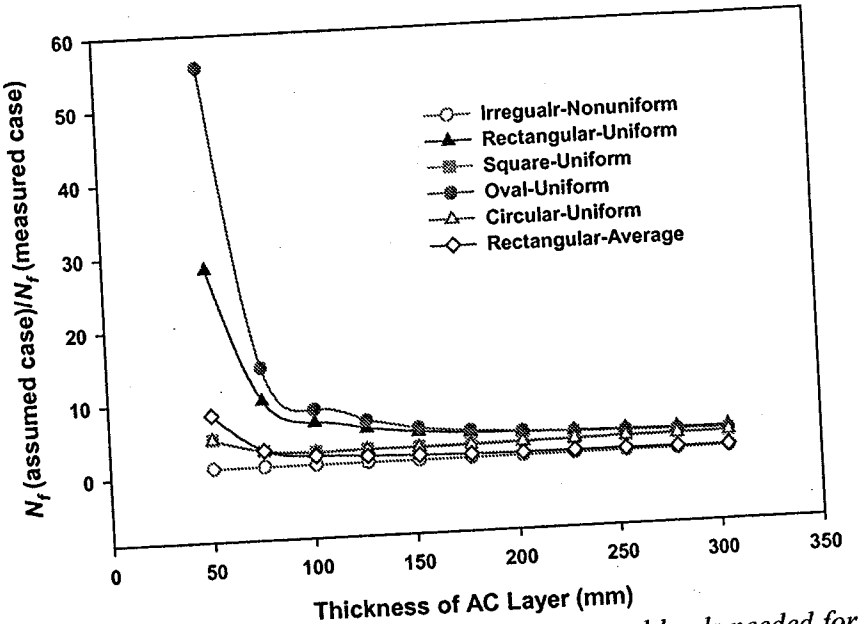

Figure 8. *Ratio between the estimated number of repeated loads needed for fatigue failure using the assumed pressure and area, and the measured pressure and area (Shell Model)*

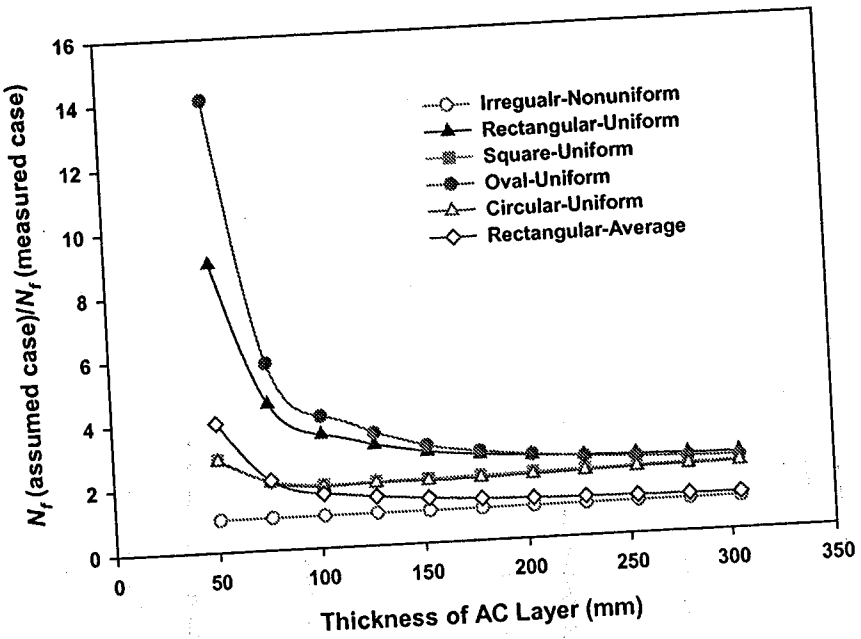

Figure 9. *Ratio between the estimated number of repeated loads needed for fatigue failure using the assumed pressure and area, and the measured pressure and area (Asphalt Institute Model)*

The effect of the calculated horizontal strains on the prediction of the number of load repetitions (N_f) fatigue cracking is shown in Figures 8 and 9. The results show that the selection of the loading configuration and geometry can significantly affect the predicted N_f value. The figures show that as the thickness of the AC layer increases the ratio between N_f values using Cases 2 through 6 and using Case 1 decreases (approaching 1). In addition, the figures indicate that the selection of the loading configuration and geometry can overpredict the fatigue life of the pavement by a factor of 56 in thin AC layers and by a factor of 7 in thick AC layers using the Shell Model. Using the Asphalt Institute Model, the fatigue life can be overpredicted by a factor of 14 in thin AC layers and a factor of 4 for thick AC layers when Cases 2 through 6 are used. It should be noted that Figures 8 and 9 do not show the ratio for the 25.4 mm AC layer due to the predicted compressive strains there.

As anticipated, the vertical strain at the top of the subgrade layer decreases with increasing AC layer thickness regardless of the load configuration and geometry, as shown in Figure 10. The results show that the vertical strains decrease as the thickness of the AC layer increases. The conventional use of the circular footprint with the tire inflation pressure (Case 5) always underestimated the vertical strains at the top of the subgrade layer while the use of the rectangular footprint with the average contact pressure (Case 6) showed relatively the best agreement in strains with Case 1. Actually, Figure 11 shows that the calculated life for rutting using Case 6 was only overpredicted by 3 percent to 8 percent while other cases overpredicted the calculated life of rutting by factors of 2.3 (Case 4), 2.6 (Case 2), 2.6 (Case 3), and 6.6 (Case 5).

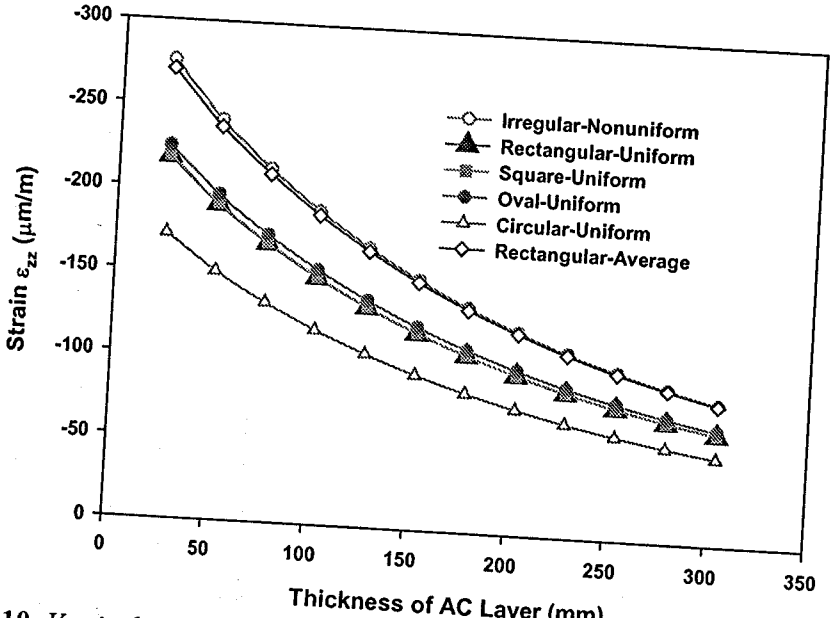

Figure 10. *Vertical strain ε_{zz} at the top of the subgrade as a function of the AC layer thickness for different loading configurations and footprint areas*

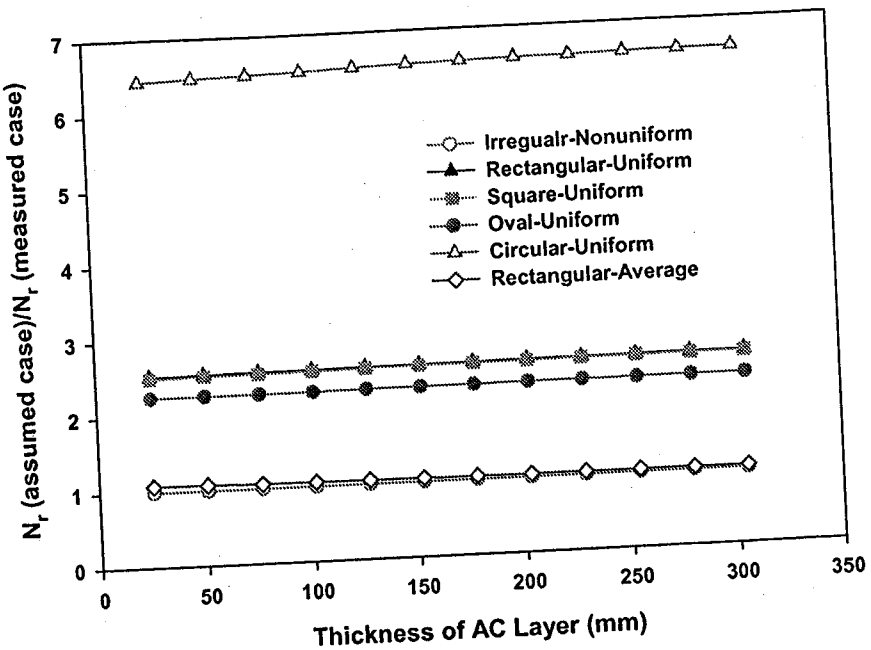

Figure 11. *Ratio between the estimated number of repeated loads needed for rutting using the assumed pressure and area, and the measured pressure and area*

4. Conclusions

Flexible pavement design and analysis depends largely on analysis performed using multilayered elastic programs. These programs are used normally to analyze layered pavement responses under circular loaded areas due to limitations in the programs to simulate actual footprint geometries and hence the reliability of the calculated pavement response should be verified. The MultiSmart3D program is a powerful multilayered program that can be used for any number of elastic layers and footprint geometry. The program was used to study the effect of the loading configuration and footprint geometry on the pavement response by varying the thickness of the AC layer.

The results of the analysis showed that the conventional footprint geometries and pressure assumptions (contact pressure is equal to tire pressure) can overpredict the fatigue and rutting life of flexible pavements. In addition, the response of the pavement system can be largely influenced by the footprint area as well as the loading configuration.

It should be noted that the presented results are applicable for the given examples only and variation in results is anticipated if different measured loading configurations and geometries are used. Therefore powerful computational tools such as the MultiSmart3D program should be utilized to predict the flexible

pavement responses using the actually measured loading configurations and geometries.

Acknowledgements

We are grateful for the support by ODOT/FHWA under grant ODOT 20943. The authors also like to thank Dr. F. Han of FWT, Inc. for helpful discussion, and the viewers for their constructive comments.

5. Bibliography

Al-Qadi I.L., M. Elseifi, and P.J. Yoo, "In-Situ Validation of Mechanistic Pavement Finite Element Modeling", *Proceedings of the 2nd International Conference on Pavement Accelerated Facilities*, B. Worel and K. Faults, Eds., Minneapolis, MN, September 26-29, 2004 (in a CD).

Beer M. (de) and Fisher C., "Contact Stresses of Pneumatic Tires Measured with the Vehicle – Road Surface Pressure Transducer Array (VSPTA) System for the University of California at Berkeley and the Nevada Automotive Test Center ", Restricted Report, Vol. I and II, University of California at Berkeley (UCB) and the Nevada Automotive Test Center (NATC), 1997.

Blab R., "Introducing Improved Loading Assumptions into Analytical Pavement Models Based on Measured Contact Stresses of Tires", *International Conference on Accelerated Pavement Testing*, Reno, NV, 1999.

Bonnaure F., Gravois A., and Udron J., "A New Method of Predicting the Fatigue Life of Bituminous Mixes", *Journal of the Association of Asphalt Paving Technologist*, Vol. 49, 1980, p. 499-529.

Hjelmstad K.D., Zuo Q.H., Kim J., "Elastic Pavement Analysis Using Infinite Elements". *Transportation Research Record 1568*, TRB, National Research Council, Washington D.C., 1997, p. 72-76.

Luo R., Prozzi J.A., "Evaluation of the Joint Effect of Wheel Load and Tire Pressure on Pavement Performance", University of Texas, Research Report SWUTC/05/167245-1, 2005.

MEPDG, National Research Council. Guide for Mechanistic-Empirical Design (MEPDG). National Cooperative Highway Research Program (NCHRP), 2004.

Pan E., "Static Response of a Transversely Isotropic and Layered Half-Space to General Dislocation Sources", *Phys. Earth Planet. Inter.*, Vol. 58, 1989a, p. 103-117.

Pan E., "Static Response of a Transversely Isotropic and Layered Half-Space to General Surface Loads", *Phys. Earth Planet. Inter.*, Vol. 54, 1989b, p. 353-363.

Pan E., "Thermoelastic Deformation of a Transversely Isotropic and Layered Half-Space by Surface Loads and Internal Sources", *Phys. Earth Planet. Inter.*, Vol. 60, 1990, p. 254-264.

Pan E., "Static Green's Functions in Multilayered Half-Spaces", *Applied Mathematical Modeling*, Vol. 21, 1997, p. 509-521.

Pan E., Alkasawneh W., and Chen E., "An Exploratory Study on Functionally Graded Materials with Application to Multilayered Pavement Design", Ohio Department of Transportation, Columbus, Ohio, Report No. FHWA/OH-2007-12, 2007.

Park D., Fernando E., Leidy J., "Evaluation of Predicted Pavement Response with Measured Tire Contact Stresses", *Transportation Research Record 1919*, TRB, National Research Council, Washington D.C., 2005, p. 160-170.

Park D.W., Martin A.E., Masad E., "Effects of Nonuniform Tire Contact Stresses on Pavement Response", *Journal of Transportation Engineering-ASCE*, Vol. 131, No. 11, 2005, p. 873-879.

Potter D.W, Donald G.S., "Revision of the NAASRA Interim Guide to Pavement thickness Design", Technical Note, Australian Road Research, Vol. 15, No. 2, June 1985.

Shook J.F., Finn F.N., Witczak M.W., Monismith C.L., "Thickness Design of Asphalt Pavements – The Asphalt Institute Method", *5th International Conference on the Structural Design of Asphalt Pavements*, Vol. 1, 1982, p. 17-44.

Skok E.L., Clyne T.R., Johnson E., Timm D.H., Brown M.L., "Best Practices for the Design and Construction of Low Volume Roads Revised", Minnesota Department of Transportation Research Services Section, November 2003 (MN/RC-2002-17REV).

Wang F., Machemehl R.B., "Mechanistic-Empirical Study of Effects of Truck Tire Pressure on Pavement: Measured Tire-Pavement Contact Stress Data", *Transportation Research Record 1947*, TRB, National Research Council, Washington D.C., 2006, p. 136-145.

Weissman S., "Influence of Tire-Pavement Contact Stress Distribution on Development of Distress Mechanisms in Pavements", *Transportation Research Record 1655*, TRB, National Research Council, Washington D.C., 1999, p. 161-167.

Yoder E.J., Witczak M.W., *Principles of Pavement Design*, John Wiley and Sons, Inc., New York, 1974.

Yue Z.Q., Svec O.J., "Effects of Tire-Pavement Contact Pressure Distributions on The Response of Asphalt Concrete Pavements", *Canadian Journal of Civil Engineering*, Vol. 22, No. 5, 1995, p. 849-860.

Received: 29 March 2007
Accepted: 16 November 2007

Road Materials and Pavement Design

Contents

Volume 9 – No. 2/2008

Papers